PERGAMON

International Journal of Heat and Mass Transfer 43 (2000) 437–445

International Journal of HEAT and MASS TRANSFER

www.elsevier.com/locate/ijhmt

Estimate of the diffusion coefficient in Co based liquids

C. Allibert[a], Ph Marty[b,*], A. Gagnoud[c], Y. Fautrelle[c]

[a]*LTPCM, BP 75, 38402 Saint Martin d'Hères, Cedex, France*
[b]*Laboratoire LEGI, BP 53 X, 38041 Grenoble, Cedex, France*
[c]*Madylam, BP 95, 38402 Saint Martin d'Hères, Cedex, France*

Received 9 November 1998; received in revised form 31 March 1999

Abstract

The experimental determination of the diffusion coefficient of given species into liquid alloys is difficult because of the unavoidable contribution of the convection. This remark applies to the case of tungsten (W) and carbon (C), introduced in liquid cobalt (Co) through the dissolution of tungsten carbide (WC). In the present work, the flow patterns produced by two different conditions of electromagnetic stirring of the liquid Co bath are computed. The electromagnetic forces which are induced by a high frequency induction coil are calculated with an integral method. They are introduced into a finite volume code for calculating the flow field. The velocity characteristics which are determined together with the experimental values of the rate constants [O. Lavergne, C. Allibert, Dissolution mechanism of WC in Co based liquids, High Temperatures, High Pressures 31 (1999)] for the dissolution of WC in the stirred liquid Co at 1450°C lead to evaluate the diffusion coefficient to 2 10^{-9} m^2 s^{-1}. It is remarkable that the values of D which are deduced for each case differ only from 14%. © 1999 Elsevier Science Ltd. All rights reserved.

Keywords: Mass transfer; Dissolution; Interface; Kinetics; Magnetohydrodynamics; Computational

1. Introduction

The cemented carbides are processed by sintering compacted powder mixtures of tungsten carbide (WC) and cobalt (Co) in the temperature range 1400–1500°C where the WC grains are surrounded by a Co rich liquid. The growth of the initial WC grain size during sintering is generally ascribed to the dissolution of the smaller grains and precipitation of the dissolved amount on the larger ones. The understanding of the overall process requires the knowledge of the elementary steps of dissolution and precipitation. In a dissolution process, the limiting step may be either the transfer of atoms from solid to liquid (interface reaction) or the transport of solute in the liquid (diffusion assisted by convection). Any stirring of the liquid accelerates the dissolution, if limited by diffusion, but does not change the kinetics if controlled by reaction. The study of the dissolution mechanism of WC in Co based liquid has been carried out by the experimental determination of the composition evolution of the liquid in equilibrium with a polycrystalline WC bar as a function of time, at 1450°C. The experimentation was done under electromagnetic stirring of the liquid. Two distinct stirring conditions, induced by two different couplers, have produced different dissolution rates. This leads to conclude to a process controlled by diffusion. The experimental details and results of this study are described in Ref. [1]. The present paper is related to the analysis of the liquid flow conditions used in Ref. [1] in order to deduce the magnitude range of the diffusion coefficient in the Co based liquid. First, the

* Corresponding author.
E-mail address: philippe.marty@hmg.inpg.fr (P. Marty)

0017-9310/00/$ - see front matter
PII: S0017-9310(99)00159-3

Nomenclature

A	vector potential of the magnetic field (Tm)	S	area of solid–liquid interface (m^2)
B	magnetic field (T)		
C	concentration (mole m^{-3})		
D	diffusion coefficient (m^2 s^{-1})		
f	electromagnetic force density (N m^{-3})	*Greek symbols*	
g	gravity (m s^{-2})	β_T	thermal expansion coefficient (K^{-1})
H	height of the liquid region (m)	β_C	concentration expansion coefficient (m^3 $mole^{-1}$)
j	electric current density (A m^{-2})	δ	electromagnetic skin depth (m)
k	dissolution rate constant (m s^{-1})	ν	kinematic viscosity of the liquid metal (m^2 s^{-1})
Re	Reynolds number: $Re = UR/\nu$	ω	angular frequency of the magnetic field (s^{-1})
r	radial coordinate (m)	Ψ	stream function (m^3 s^{-1})
Sh	Sherwood number; $Sh = k(H/2)/D$	ρ	density of the liquid metal (kg m^{-3})
T	temperature (K)	σ	electrical conductivity (Ω^{-1} m^{-1})
t	time (s)	τ	shear stress (Pa)
U	velocity scale (m s^{-1})	θ	angular coordinate
U^*	friction velocity (m s^{-1})	φ	electric potential (V)
u	velocity component (m s^{-1})		
V	volume of liquid metal (m^3)		
Sc	Schmidt number; $Sc = \nu/D$		

force field and the velocity field are computed for each of the two experiments, giving rise to a turbulent and a laminar flow, respectively. Then, the diffusion coefficient is estimated from the characteristic values of the velocity.

2. Experimental determination of the dissolution rate constant

2.1. Description of the experimental facility

The experiments have been done on the facility shown in Fig. 1 which consists of a WC inner cylinder with a radius equal to 10 mm surrounded by liquid cobalt contained in an alumina crucible having an inner radius of 22 mm. The height of the annular liquid region is equal to $H = 28$ mm. The electromagnetic heating and stirring are induced by a 12-turn coil supplied with a 10 khz electric current. The heat transfer coupling is enhanced by supplying an electromagnetic coupler between the alumina crucible and the coil. Two types of couplers were used: a graphite crucible, with a wall thickness 9 mm and a molybdenum crucible, with a wall thickness 5 mm. Table 1 shows the physical properties of the various materials used in each experiment. The graphite coupler for which the electromagnetic skin depth, δ_{em}, is equal to 27 mm at 10 khz, enables a good penetration of the magnetic field in the liquid cobalt as well as a strong stirring. With the molybdenum coupler $\delta_{em} = 1.1$ mm : most of the heating is made in the coupler and the electromagnetic forces in the liquid cobalt are expected much smaller than in the previous case. The current intensity in the coil is 350 A with the graphite coupler and is equal to 525 A with the molybdenum coupler. The mean temperature of the experiment is 1450°C.

2.2. Dissolution rate constants

The experimental results described in [1] show an equivalent increase of the carbon and tungsten con-

Table 1
Physical properties of the different materials used in the dissolution experiment shown in Fig. 1

	Electrical conductivity σ (Ω^{-1} m^{-1})	Density ρ (kg m^{-3})	Kinematic viscosity ν (m^2 s^{-1})
Solid WC	5.6×10^6	15,800	
Graphite coupler	3.3×10^4	1500	
Molybdenum coupler	18.8×10^6	10,000	
Liquid cobalt	0.98×10^6	8600	10^{-7}

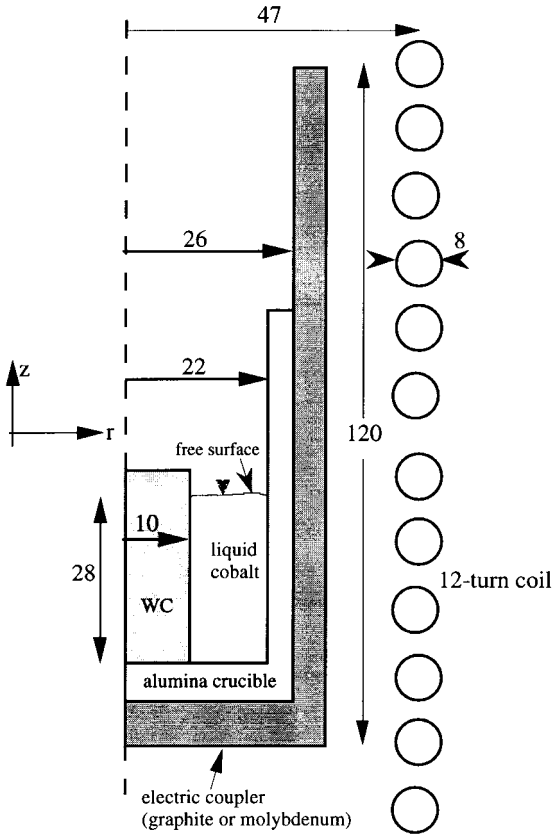

Fig. 1. Experimental facility for the measurement of the dissolution rate of WC in liquid cobalt (all dimensions in mm).

tents dissolved in the liquid. As shown in Fig. 2, the time dependence of the C and W concentrations is very correctly represented by the equations:

$$V\frac{dC}{dt} = kS(C^* - C) \tag{1}$$

integrated as:

$$\ln\frac{C^* - C_0}{C^* - C} = \frac{S}{V}kt \tag{2}$$

where C^*, C_0 and C are, respectively, the W or C contents corresponding to the solubility limit, the initial and instant values. S is the area of the solid–liquid interface, V is the liquid volume, k is the dissolution rate constant and t is the dissolution time.

This model expresses the variation of flux of the solute species through the solid–liquid interface as proportional to the change of species concentration in the liquid, as usually described for diffusion through a film. It assumes a linear gradient of solute content (C^*-C) in a boundary layer of thickness δ, along the solid–liquid interface, and a constant instant content C in the other part of the liquid. This model, that corresponds to a liquid perfectly homogenised by stirring, relates the dissolution rate constant k to the diffusion coefficient D by:

$$k = D/\delta.$$

The values of k deduced from the experimental results [1] are:

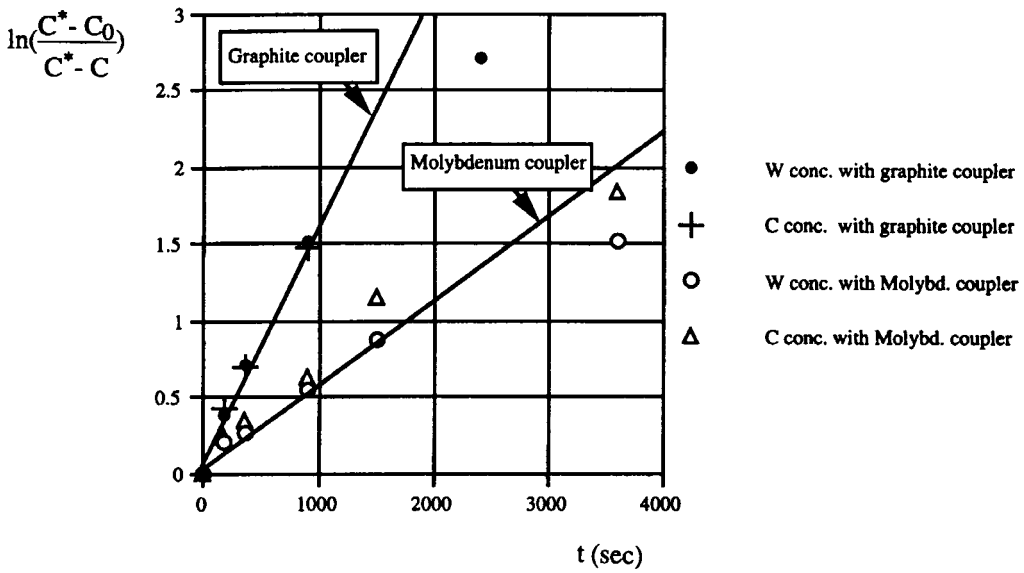

Fig. 2. Time dependence of the concentrations of carbon (C) and tungsten (W) in liquid Co at 1450°C. The ratio V/S is 3.11×10^{-2} m for the graphite coupler and is 2.9×10^{-2} m for the molybdenum coupler.

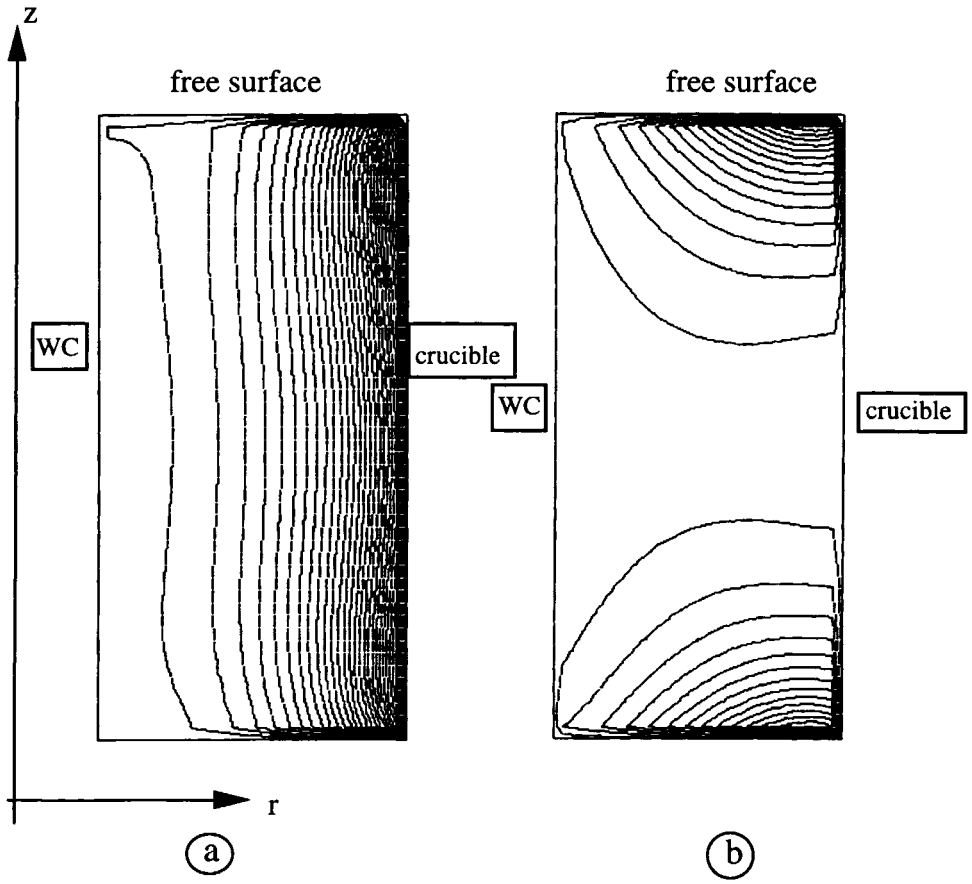

Fig. 3. Iso contours of the radial (a) and axial (b) forces for the case of a graphite coupler.

$$k_1 = 4.9\ 10^{-5}\ \mathrm{m\ s^{-1}} \tag{3}$$

and

$$k_2 = 1.6\ 10^{-5}\ \mathrm{m\ s^{-1}} \tag{4}$$

for the graphite and molybdenum coupler, respectively. Such values compare with those determined for the dissolution of TiC in liquid Co [2], by the technique of the rotating disk, usually employed for a dissolution kinetics study.

3. Flow computation

As the magnetic field distribution is unaffected by the liquid metal flow, it is therefore possible to calculate the magnetic field in a quasi-static approximation and to introduce the associated force field in the momentum equations.

3.1. Force field calculation

In the axisymmetric approximation, the magnetic field distribution $\vec{B} = (B_r,\ 0,\ B_z)$ can be deduced from the azimuthal component, A_θ, of the vector potential $\vec{A}$ defined as:

$$\vec{B} = \mathrm{curl}\ \vec{A} \tag{5}$$

The component A_θ, which is the only non-zero component of the vector potential, is linked to the electric current density, j_θ, in every conducting part by Ohm's law:

$$j_\theta = -\sigma\left(\frac{\partial \phi}{r\,\partial \theta} + \frac{\partial A_\theta}{\partial t}\right) \tag{6}$$

where $\partial\phi/r\,\partial\theta$ stands for the azimuthal gradient of electric potential imposed to the coil and t denotes the time. This gradient is zero inside the liquid metal load

as well as in the conducting walls. The integral method described in [3] has been used to solve the problem. This method takes advantage of the sinusoidal nature of the electric variables which allows to write:

$$\frac{\partial A_\theta}{\partial t} = i\omega A_\theta \tag{7}$$

and of the Biot and Savart relation between the current density and the vector potential:

$$A_\theta = \frac{\mu_0}{4\pi}\int\int\int \frac{j}{r}\,\mathrm{d}v \tag{8}$$

where μ_0 is the magnetic permeability of vacuum, r is the distance between the current sources and the point where A_θ is to be calculated and $\mathrm{d}v$ stands for the elementary volume. For a given gradient of electric potential, Eqs. (6)–(8), are combined to yield a linear system which solution gives j everywhere in the coil and in the other conducting parts. The vector potential and hence, $\vec{B}$, is obtained from this result. The averaged value of the electromagnetic force $\vec{j}\times\vec{B}$ over a period of the electric current is finally calculated.

Fig. 3(a) and (b) show the force distribution in the liquid region when the graphite coupler is used with a current intensity equal to 350 A. Owing to axisymmetry, the azimuthal component f_θ is zero. The radial, inward directed, force f_r is almost z-independent and decreases from 250,000 N m^{-3} along the external radius to 0 near the WC–Co interface. The vertical force f_z is positive in the bottom of the annulus and negative near the free surface. Its absolute value is around 150,000 N m^{-3}. When the molybdenum coupler is used, the force pattern remains almost unchanged but the typical values of the forces are much less: the intensity of the radial force is only 2800 N m^{-3} whereas that of the axial force ranges between $+920$ N m^{-3} near the bottom to -1500 N m^{-3} near the free surface. This strong decrease is due to the large shielding of the magnetic field by the molybdenum coupler.

3.2. Velocity field computation

The force field (f_r, 0, f_z) is introduced in the commercial finite volume solver FLUENT to obtain the flow pattern. Usual no-slip conditions are imposed along solid boundaries ($\vec{U}=0$) whereas free-slip conditions are prescribed at the free surface which is assumed to remain horizontal:

$$\frac{\partial u_r}{\partial z} = u_z = 0 \quad \text{at the free surface.} \tag{9}$$

A 30×50 mesh has been used in the radial and vertical directions, respectively. When required, a standard $k-\epsilon$ turbulence model has been used (here k denotes the kinetic energy of turbulence and ϵ its rate of dissipation). Visualisation of the meridional velocity streamlines (u_r, 0, u_z) is made through iso-contour plots of the streamfunction Ψ defined as:

$$(u_r, 0, u_z) = \mathrm{curl}\left(0, \frac{\Psi}{r}, 0\right). \tag{10}$$

3.3. Estimation of the thermal or solutal convection velocity

As our calculations neglect the influence of thermal or solutal convection, it is necessary to estimate the order of magnitude of the associated velocities.

Assuming a balance between inertia and thermal buoyancy forces gives:

$$\frac{\rho U_\mathrm{T}^2}{l} \approx \rho g \beta_\mathrm{T} \Delta T \tag{11}$$

where U_T is a typical velocity which would be induced by thermal convection alone, l is a typical dimension, eg. the radial distance between the inner and the outer walls, β_T is the volumetric expansion coefficient and ΔT an order of magnitude of the temperature difference in the bath. Introducing the numerical values: $l = 12\times 10^{-3}$ m, $\beta_\mathrm{T} = 10^{-4}$ K^{-1}, $\Delta\mathrm{T} = 10$ K, in Eq. (11) gives:

$$U_\mathrm{T} \approx 0.01 \text{ m/s}.$$

The same approach gives an estimation of the solutal velocity, U_S, which would appear owing to the difference in the concentrations of W and C in the liquid cobalt:

$$\frac{\rho U_\mathrm{S}^2}{l} \approx \rho g \beta_\mathrm{S} \Delta C \tag{12}$$

where β_S is the solutal expansion coefficient and ΔC a typical concentration difference in the bath. Introducing the estimated values: $\beta_\mathrm{S}\Delta C \approx 10^{-3}$ in Eq. (12) gives:

$$U_\mathrm{S} \approx 0.01 \text{ m/s}.$$

The velocity fields U_T and U_S have the same order of magnitude and the value 0.01 m/s should be kept in mind when examining the results of the following section.

4. Results

Two different cases are considered according to the characteristics of the electromagnetic coupler which

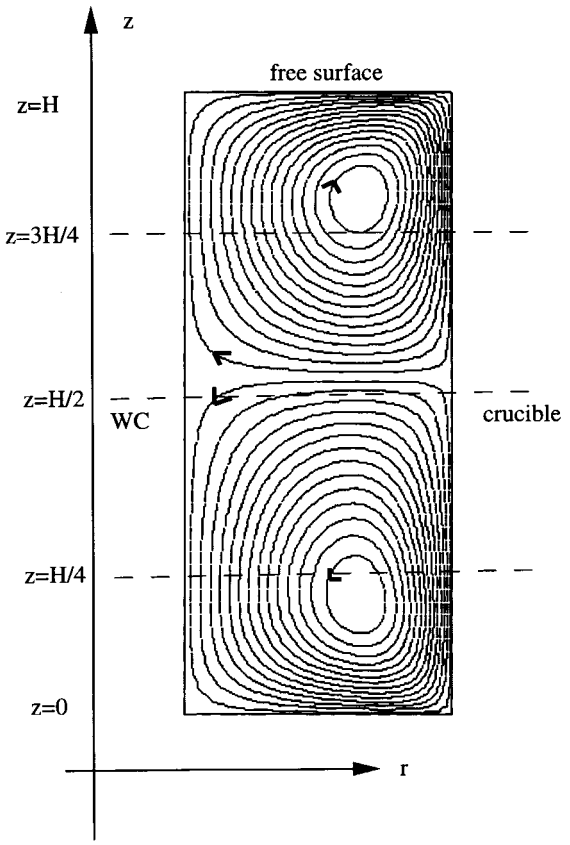

Fig. 4. Case 1 (graphite coupler): iso-contours of the stream-function Ψ of the flow.

has been used. These two cases will be referred to as Case 1 and 2, respectively. For each case, we will try to deduce the value of the diffusion coefficient, D, or, equivalently, that of the Schmidt number, Sc.

4.1. Case 1: graphite coupler

As mentioned previously, the magnetic field is only weakly damped by the coupler and a rather intense turbulent stirring is produced. The streamlines are shown on Fig. 4 and display two meridional counter-rotating rolls, the one at the top rotating in the clockwise direction. Owing to the difference between the boundary conditions at the bottom of the bath where $\vec{U}=0$ is imposed and at the free surface, these two rolls are slightly different. The maximum velocity in the whole bath is found equal to $U_m=0.295$ m s^{-1}. It is here important to remark that this velocity is about 30 times that found for the thermal or solutal convection velocity. The regions where the velocity is higher than 0.2 m s^{-1} (Fig. 5) are concentrated near outer top and bottom corners of the liquid zone. These regions correspond to the highest values of the electromagnetic

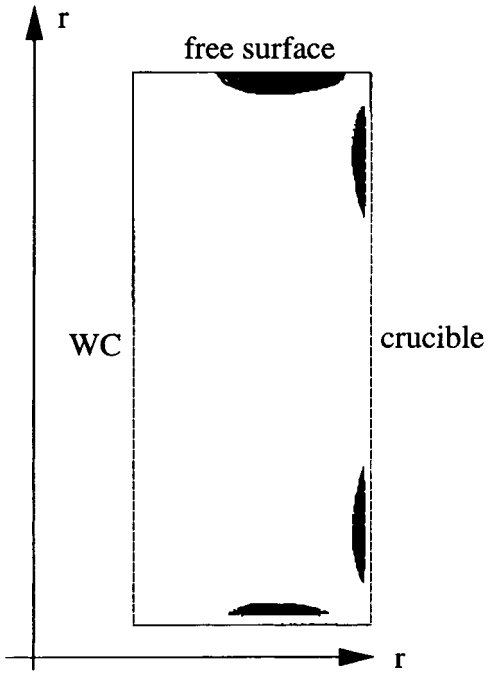

Fig. 5. Case 1 (graphite coupler): iso-contour of Ψ showing the regions where the velocity is higher than 0.2 m s^{-1}.

forces. The mean flow is turbulent and develops thin boundary layers along the two vertical solid walls. This is shown in Fig. 6 which displays three radial profiles of the vertical velocity v_z at the altitudes defined in Fig. 4. Two of them cross each one of the two vortices near its center whereas the third one is plotted at the mid-height of the bath. Fig. 7 outlines the profile

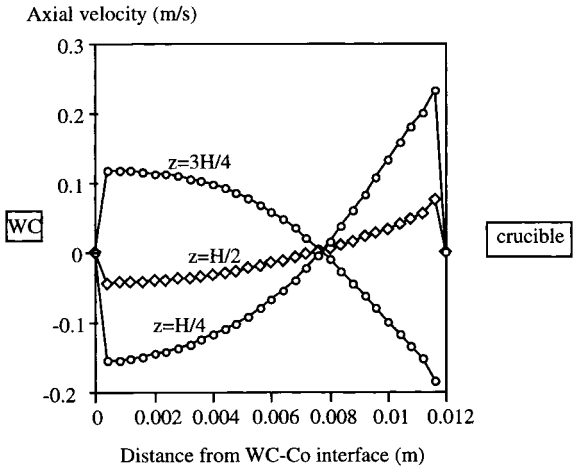

Fig. 6. Case 1 (graphite coupler): radial profiles of the vertical velocity u_z at three different heights (see Fig. 4).

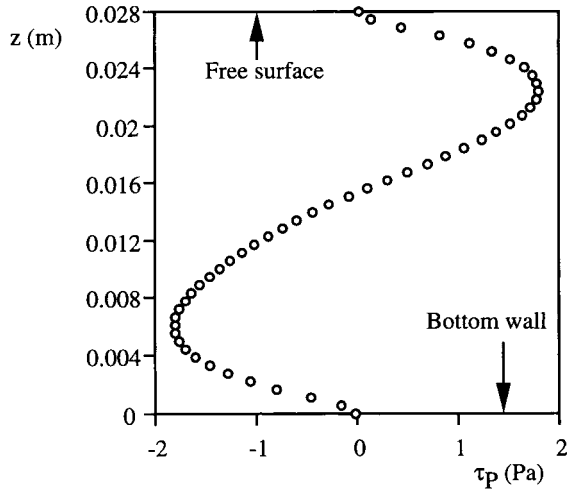

Fig. 7. Case 1 (graphite coupler): wall friction τ_P along the WC–Co interface.

of the turbulent friction velocity U^* along the WC–Co interface. This velocity is defined as:

$$U^* = \sqrt{\frac{\tau_P}{\rho}} \tag{13}$$

where τ_P is the wall shear stress and ρ is the fluid density. The velocity U^* follows a sinus-like distribution similar to the magnitude of the velocity u_z in this region. Its mean value $\overline{U^*}$ along the vertical interface can be approximated as follows:

$$\overline{U^*} = \overline{\sqrt{\frac{|\tau_P|}{\rho}}} = \overline{\sqrt{\frac{\tau_{max}}{\rho}\sin\frac{z\pi}{H/2}}} \tag{14}$$

where $H = 28$ mm is the liquid depth and $\tau_{max} = 1.8$ Pa is the maximum value of the tangential shear deduced from Fig. 7. One finally finds:

$$\overline{U^*} = 0.009\ \mathrm{m\ s^{-1}}. \tag{15}$$

The diffusion coefficient, D, is linked to the dissolution rate, k_1, by the Sherwood number:

$$Sh = \frac{k_1 H/2}{D} \tag{16}$$

which represents the ratio of the mass flux carried by convection to that ensured by diffusion. Here, Sh is built with the mid-height $H/2$[1] of the bath. Then, in order to calculate D, we need to deduce Sh from the turbulent characteristics of the flow. In this respect, the results available for heat exchanges in circular ducts [4] can be extended to this mass transfer problem. We obtain:

$$Sh = \frac{6}{25}\frac{ReSc(U^*/U)}{Sc + \ln(1+5Sc) + 0.5\ \ln\left(\frac{Re(U^*/U)}{60}\right)} \tag{17}$$

Using the maximum velocity $U_m = 0.295$ m s^{-1} and still $H/2 = 0.014$ m as characteristic velocity and length scales, respectively, give $Re = 41{,}300$ and $U^*/U = 0.03$. This latter value is in agreement with well-known investigations of the turbulent boundary layer along a flat wall [5] where it is found that: $U^*/U \approx 1/30$.

The value of Sc is still unknown but can be foreseen to be very large compared to unity. This allows to simplify Eq. (17) to:

$$Sh = \frac{6}{25}Re\frac{U^*}{U} \tag{18}$$

with an error equal to 12% when $Sc = 50$ and 6% only when $Sc = 100$.

From Eqs. (16) and (18) we find:

$$D = 2.3 \times 10^{-9}\ \mathrm{m^2\ s^{-1}} \tag{19}$$

which gives the value of Sc:

$$Sc = 43. \tag{20}$$

4.1. Case 2: molybdenum coupler

In this case, the magnetic field is strongly reduced and the flow remains laminar.

Fig. 8 shows the corresponding streamlines which strongly resemble those obtained in Case 1. The regions with the highest velocity are still located near the top and bottom external corners. Nevertheless, the velocity magnitude is much smaller and reaches a peak value at 0.029 m s^{-1}, i.e. 10 times less than in Case 1. This velocity is nevertheless still 3 times larger than that estimated for the thermal or solutal velocity.

Building the Reynolds number of this flow with the distance between the inner and the outer interfaces which limit the annular liquid region gives:

$$Re \approx 3400 \tag{21}$$

This value suggests a laminar and stationary flow, what is confirmed by the good convergence of the numerical code when a laminar model is used. As in Case 1, Fig. 9 shows horizontal profiles of the vertical velocity through each meridional cells and through the

[1] $H/2$ equal 14 mm and is quite comparable to the radial extent of the annular liquid region. The latter is 12 mm wide and could also have been used as a typical length scale.

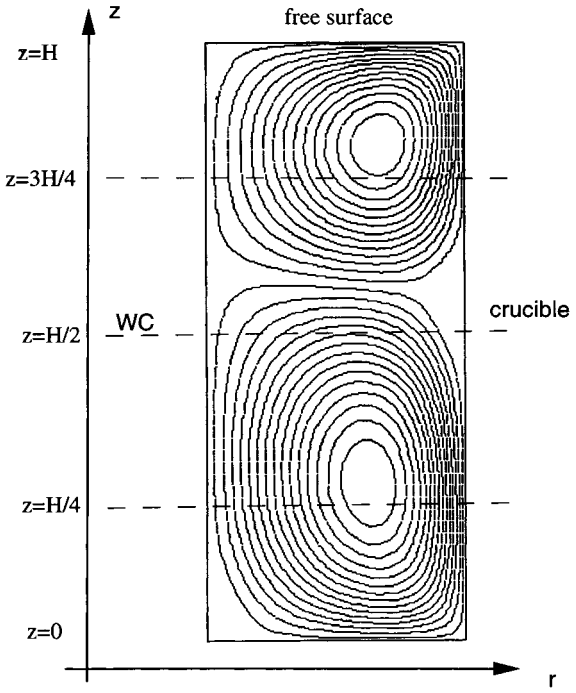

Fig. 8. Case 2 (molybdenum coupler): iso-contours of the streamfunction Ψ of the flow.

mid-height plane. As expected from this low Reynolds number situation, the vertical walls boundary layer thickness is higher than in Case 1 and the mean velocity far away from the WC–Co interface is roughly equal[2] to 0.015 m s^{-1}. In order to deduce the value of the diffusion coefficient, D, from this second experiment, we write a definition of the Sherwood number similar to that of Eq. (16):

$$Sh = \frac{k_2 H/2}{D}. \tag{22}$$

In this situation where the Schmidt number is much greater than unity, the Sherwood number can be estimated from the expression available for a laminar flow over a flat plate:

$$Sh = 0.66(Re_{H/2})^{1/2} Sc^{1/3} \tag{23}$$

where the Reynolds number $Re_{H/2}$ is built with the velocity in the outer region of the interface boundary layer previously defined ($U_\infty = 0.015$ m s^{-1}) and with the half-height, ($H/2 = 0.014$ m) of the bath. Introducing the experimental value $k_2 = 1.6 \times 10^{-5}$ m

[2] This value is the average between the absolute value of the velocity in the bottom region, where $u_z \approx 0.02$ m s^{-1}, and in the top, where $u_z \simeq 0.01$ m s^{-1}.

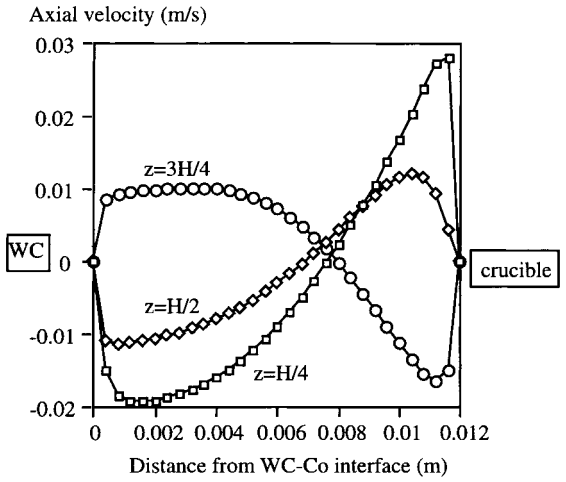

Fig. 9. Case 2 (molybdenum coupler): horizontal profiles of the vertical velocity u_z at the same positions as in Fig. 6.

s^{-1} from Eq. (4) gives:

$$Sc = 50 \tag{24}$$

corresponding to:

$$D = 2 \times 10^{-9} \text{ m}^2 \text{ s}^{-1} \tag{25}$$

what is in global agreement with the value previously found in Eq. (20) and then confirms the negligible contribution of the solute or thermal convection.

5. Conclusion

The experimental determination of diffusion data in liquids is difficult because of the contribution of the thermal or solutal convection to the total mass transport. Consequently, the techniques involving controlled convection are preferably used. As reported in the review on the diffusion in liquid metals, by Kubicek and Peprica [6], the electromagnetic stirring enables only a rough evaluation of the convection contribution and of the diffusion coefficients. The present results exhibit a good consistency between the Schmidt number and the diffusion coefficient values deduced from the two conditions of laminar and turbulent flows used for their determination. Consequently, the computation of the liquid flow pattern produced by electromagnetic stirring, associated to the experimental determination of dissolution rate constants in electromagnetically stirred liquids provide an approach for the evaluation of diffusion coefficient, mainly valuable for the systems involving high temperature investigations.

As for the diffusion coefficient value, D, it is in the

magnitude range found in literature for most of refractory metals in liquid Fe or Fe,C alloys. The literature review [7] on the diffusion of several metals M and of C in liquid alloys (Fe, M, C) reports the ranges (2–5) $\times 10^{-9}$ and (10–20) $\times 10^{-9}$ m^2 s^{-1} for the diffusion of M and C, respectively. While these values are not drastically different, they indicate a diffusion slightly more rapid for C than for M. The few data published on the diffusion of W in Ni [8] and Ti in Co [2], respectively, 10^{-8} and 10^{-10} m^2 s^{-1}, indicate a similar behaviour for the solvents Fe, Ni and Co. When compared to the literature, the value of D presently obtained (2×10^{-9} m^2 s^{-1}) leads to conclude that the dissolution of WC is limited by diffusion of W in the Co based liquid.

References

[1] O. Lavergne, C. Allibert, Dissolution mechanism of WC in Co based liquids, High Temperatures, High Pressures 31 (1999).

[2] V.N. Eremenko, M.M. Churakov, Dissolution rate of TiC in molten Co, Fiz-Khim. Mekhanika Mater. 6 (3) (1970) 62–67.

[3] A. Gagnoud, B. Maestrali, P. Masse, Modelling of motion in liquid metal limited by a free surface and a solidification front, Eur. J. Mech. B/Fluids 10 (5) (1991) 552–562.

[4] C. Burmeister, Convective Heat Transfer, Wiley, New York, 1993.

[5] H. Schlichting, Boundary Layer Theory, McGraw-Hill, New York, 1951.

[6] P. Kubicek, T. Peprica, Diffusion in molten metals and melts: applications to diffusion in molten iron, Inter. Met. Rev. 28 (3) (1983) 131–157.

[7] C.H. Allibert, Diffusion behaviour in the Co based liquids, CERMeP Contract Report 1996-01, 1-11, 1996.

[8] A.V. Natanzon, B.P. Titov, P.B. Antonchenko, Solubility and dissolution kinetics of W in Ni at 1525°C, Porosch. Met. 2 (1992) 73–77.